ISSN: 2458-8989

Natural and Engineering Sciences

NESciences, 2026, 11 (3): 178-200 doi: 10.28978/nesciences.263016

Antiviral Potential of Alpinia purpurata Against DENV-4: Integrated In Vitro and In Silico Evaluation of Non-Structural Protein Inhibition

Mochammad Aqilah Herdiansyah[1], Win Darmanto[2]*, Dwi Winarni[2], Ruey-an Doong[3], Mochamad Radika Tory Alifiansyah[4], Putri Ayu Ika Setiyowati[1], Aulia Umi Rohmatika[5], Tri Widiandani[6,7,8]

[1]Doctoral Program of Mathematics and Natural Sciences, Faculty of Science and Technology, Universitas Airlangga, Surabaya, Indonesia.

[2]Department of Biology, Faculty of Science and Technology, Universitas Airlangga, Surabaya 60115, Indonesia.

[3]Institute of Analytical and Environmental Sciences, National Tsing Hua University, Sec. 2 Kuang Fu Road, Hsinchu 30013, Taiwan.

[4]Master of Pharmaceutical Sciences, Faculty of Pharmacy, Universitas Airlangga, Surabaya, Indonesia.

[5]Faculty of Medicine, Universitas Pembangunan Nasional Veteran, Surabaya, East Java, Indonesia.

[6]Department of Pharmaceutical Sciences, Faculty of Pharmacy, Universitas Airlangga, Surabaya 60115, Indonesia.

[7]Research Group of Drug Development, Faculty of Pharmacy, Universitas Airlangga, Surabaya 60115, Indonesia.

[8]Inter-University Center of Excellence (IUCoE) of Health Autonomy-Drug Discovery, Universitas Airlangga, Surabaya, Indonesia.

Abstract

Despite its unique structural characteristics and the limited availability of effective therapeutics options, dengue virus serotype 4 (DENV-4) remains relatively underexplored. This study investigates the antiviral potential of Alpinia purpurata ethanol extract against DENV-4 through an integrated in vitro and in silico approach targeting non-structural proteins (NS1, NS3 helicase, and NS5). The extract was prepared by ethanol maceration, and its antiviral efficacy was evaluated by determining cytopathic effects and half-maximal effective concentration (EC_{50}) using a Viral ToxGlo™ assay in DENV-4-infected Vero E6 cells. Cytotoxicity was assessed by MTT assay in Vero E6 cells, and the selectivity index (SI) was determined based on the CC_{50} and EC_{50} values. Computational analyses included phytochemical exploration, drug-likeness prediction, molecular docking, molecular dynamics simulations, ADME assessment, and toxicity profiling. At higher concentrations, the extract reduced cytopathic effects from 78.82% to 4.79% in a concentration-dependent manner and exhibited antiviral activity with an EC_{50} value of 92.38 µg/mL. Cytotoxicity assessment using the MTT assay revealed a CC_{50} value of 137.77 µg/mL, resulting in a SI of 1.49. In silico analyses identified phenolic compounds, particularly epicatechin, as the most promising candidates, exhibiting strong binding affinities toward NS1 (-4.27 kcal/mol), NS3 helicase (-7.00 kcal/mol), and NS5 (-6.14 kcal/mol). Notably, epicatechin

*Corresponding Author: Win Darmanto, Email: windarmanto@fst.unair.ac.id

outperformed the reference compound quercetin in its interaction with NS3 helicase. Molecular dynamics simulations confirmed the stability of ligand-protein interactions, particularly within the NS3 helicase complex, which also exhibited favorable binding free-energy profiles. ADME and toxicity predictions indicated favorable pharmacokinetic properties and a generally low toxicity profile. Collectively, these findings identify epicatechin as a promising multitarget inhibitor of key viral replication proteins and demonstrate the moderate yet significant anti-DENV-4 activity of A. purpurata extract. These findings highlight the potential of Indonesian medicinal plants as sources of antiviral agents and provide a foundation for future in vivo investigations and antiviral drug development.

Keywords
Alpinia purpurata, Dengue virus serotype-4 (DENV-4), Epicatechin, In vitro-in silico approach, Multitarget inhibition,

Available Online: 01/09/2026

Introduction

One of the most severe infectious diseases transmitted by Aedes aegypti mosquitoes in the globe is dengue hemorrhagic fever (DHF). DENV-1, DENV-2, DENV-3, and DENV-4 are the four serotypes of the dengue virus that cause this illness. The efficiency of anti-dengue interventions still varies among serotypes, especially against DENV-4, which tends to demonstrate a poorer immune response and has minimal clinical data, despite extensive immunization efforts by academics and medical experts. According to Kiemel et al. (2024), there isn't yet a specific and effective antiviral drug that can prevent the dengue virus from spreading.

Although DENV-4 has historically received less attention than DENV-1 and DENV-2, recent epidemiological trends indicate its increasing public health relevance. Global dengue transmission reached unpredented levels in 2024, with more than 14 million reported cases worldwide, representing the largest dengue outbreak ever recorded. The emergence and co-circulation of multiple serotypes, including DENV-4, have been increasingly reported in endemic regions, raising concerns regarding severe disease outcomes associated with secondary heterologous infections and antibody-dependent enhancement (ADE). Moreover, recent surveillance data demonstrated a growing proportion of DENV-4 infections in several outbreak settings, highlighting its expanding circulation and epidemiological significance (World Health Organization, 2025). Despite of this trend, DENV-4 remains comparatively understudied, particularly regarding antiviral discovery and molecular target characterization. Furthermore, no specific antiviral therapy has yet been approved for dengue infection, and current clinical management remains largely supportive. These gaps underscore the urgent need to identify novel antiviral candidates targeting DENV-4 replication and pathogenesis.

One of the most promising strategies for creating antidengue drugs it to target non-structural (NS) proteins, which are crucial for encoding the processes of dengue virus replication and assembly. Numerous non-structural protein types have been identified, such as NS1, NS3 helicase, and NS5. The NS1 protein is known to have an impact on immune system regulation and vascular pathology. Furthermore, the NS3 helicase is necessary for unwinding viral RNA during replication, while the NS5 protein function as an RNA-dependent RNA polymerase (RdRp) and methyltransferase involved in RNA synthesis and protection of the viral genome from host enzymatic degradation (Halim et al., 2017)

In vitro and in silico techniques have been widely employed to identify natural compounds that can inhibit the function of dengue non-structural proteins. According to a recent study by Bharadwaj et al. (2019), bioactive compounds from Azadirachta indica and Ganoderma lucidum effectively inhibit the NS2B-NS3 protease complex, reducing viral infectivity. Furthermore, through stable and non-toxic interactions, Islam et al. (2024) discovered via an in silico analyses that natural compounds from medicinal plants could effectively limit the activity of the NS3 protease-helicase complex.

One tropical plant with great potential that hasn't been fully studied as an antidengue agent is Alpinia purpurata, also known as red ginger lily. This plant is rich in flavonoids, phenolics, and terpenoids, which have strong antiviral, antiinflamatory, and antioxidant activites against several RNA viruses (Lee et al., 2023). The ethanol extract of A. purpurata has excellent antioxidant activity because it can scavenge free radicals and boost the expression of endogenous antioxidant enzymes including superoxide dismutase (SOD) and catalase (CAT). In order to avoid oxidative stress, which can worsen dengue virus infection in host cells, this antioxidant activity is essential (Cheng et al., 2017). Furthermore, it has been found that phenolic and terpenoid compounds reduce the expression of pro-

inflammatory cytokines and block the NF-κB signaling pathway, which is known to contribute to inflammatory responses after DENV infection (Kairat et al., 2024). Additionally, A. purpurata extract has demonstrated cytoprotective and antiproliferative activities through routes like cell cycle arrest and apoptosis induction in cancer cells without appreciably damaging healthy cells (Mesmar et al., 2022). These activites enhance the safety and therapeutic potential of A. purpurata extract for in vitro studies using Vero E6 cells, which are commonly utilized in DENV antiviral research.

The current research gap remains focused on DENV-2 or mixed serotypes, whereas DENV-4 possesses unique structural variations in its non-structural proteins that may influence the effectiveness of inhibitors. In addition, there is a lack of exploration of local natural resources, such as A. purpurata, for anti-dengue purposes, even though this plant is an endemic tropical species in Indonesia and contains various potentially bioactive compounds that have not yet been tested against dengue non-structural proteins. Furthermore, integrative studies combining in silico approaches (molecular docking and dynamic simulation) with in vitro validation of the effectiveness of natural compounds against DENV-4 target proteins remain limited. Therefore, this study aims to investigates the antiviral potential of A. purpurata ethanol extract against DENV-4 through an integrated in vitro and in silico approach targeting non-structural proteins (NS1, NS3 helicase, and NS5).

To the best of our knowledge, this study is the first to comprehensively investigate the anti-DENV-4 potential of A. purpurata through the integration of experimental antiviral validation and multitarget computational analyses. Previous studies on A. purpurata have primarily focused on its phytochemical composition and general biological activities, while its activity against DENV-4 and its interactions with key viral non-structural proteins remain largely unexplored. The novelty of the present work lies in the combination of DENV-4-specific antiviral screening with comprehensive in silico evaluation of phytochemical constituents against multiple viral replication targets, including NS1, NS3 helicase, and NS5. Furthermore, molecular dynamics simulations, ADME profiling, and toxicity assessments were integrated to identify promising lead compounds and elucidate their potential mechanism of action. Therefore, this study is expected to provide new insights for the development of anti-dengue candidates from A. purpurata targeting non-structural proteins involved in viral replication.

Materials and Methods

Sample collection and preparation of extract

Rhizome samples of A. purpurata were collected from Tanjung Market, Mojokerto City, East Java, Indonesia (latitude: 7°28'1"S; longitude: 112°26'12"E). The extraction process began with cutting the rhizomes, which were then air-dried for 14 days. 96% ethanol was used as a solvent in a 1:3 (w/v) ratio to macerate the dried material. For seven days in a row, the mixture was agitated twice a day, and the solvent was changed anytime the extract grew too thick. The goal of this process was to extract as many secondary metabolites as possible from the rhizome of A. purpurata. After filtering the macerate, the residue was extracted again using the same method. Subsequently, the filtrate was evaporated using a rotary evaporator at a temperature of 40–60 °C, a rotation speed of 80–120 rpm, and a vacuum pressure of 100–200 mbar. The resulting concentrated extract was scraped off and stored in sample vials for further use. The extraction yield was calculated based on the ratio between the weight of the dried crude extract and the initial dry plant material weight. From 2,0 kg of dried rhizome powder, 60 g of crude ethanol extract was obtained, corresponding to an extraction yield of 3,0% (w/w). All subsequent in vitro experiments were conducted using the single extraction batch to minimize variability associated with extraction procedures.

Preparation of Vero E6 cells and virus culture

Vero E6 cell cultures (ATCC® CRL-1586™) (Merck, USA) were employed as the experimental model and obtained from the Institute of Tropical Diseases, Universitas Airlangga, Indonesia. Cells were maintained in Dulbecco's Modified Eagle's Medium (DMEM; Merck, USA) supplemented with 10% fetal bovine serum (FBS; Merck, USA) and 1% penicillin-streptomycin. The cultures were incubated at 37°C in a humidified atmosphere containing 5% CO_2. The DENV-4 strain (Acc. No. KT204464) used in this study was kindly provided by the Dengue Laboratory, Institute of Tropical Diseases, Universitas Airlangga, Indonesia.

Antidengue replication assay

The evaluation of anti-dengue replication activity was conducted using the Viral ToxGlo™ Assay to determine the EC_{50} value and the percentage of cytopathic effect. 96-well flat-bottom luminescence

microplates were used for the assay. Four treatment groups were used in the experiment: medium control, cell control, DENV-4 control, and sample-treated groups. Before treatment, the medium in the 96-well flat-bottom luminescence plate was disposed of. Each well in the medium control and cell control groups received 50 µL of MEM supplemented with 10% FBS, whereas the labeled sample wells received 25 µL. Every concentration was examined three times. The corresponding wells were then filled with 50 µL of DENV control and 25 µL of DENV-4 stock solution (2×10^3 FFU/mL). The microplates were incubated for 48–144 hours at 37 °C in a humidified atmosphere containing 5% CO_2. After incubation, 100 µL of the Viral ToxGlo™ assay reagent was added to each well and further incubated for 10 minutes under the same conditions (37 °C, 5% CO_2). Luminescence readings were then measured using a GloMax® microplate reader (Wiradana et al., 2025).

Cytotoxicity assay

The cytotoxicity test of crude extract A. purpurata on Vero E6 cells was performed using the MTT assay. Vero cells ($5x10^4$ cells/ml) were seeded in a 96-well plate and treated with A. purpurata extract at various concentrations (50 ppm, 100 ppm, 150 ppm) in triplicate. The cells were incubated for four days at 37°C and 5% CO_2. At the end of the incubation phase, 15 µL of MTT solution (Promega, WI, USA) was added to each well. The microplate was placed at 37°C for 4 hours, accompanied by the addition of 100 µL of stop mix solution to each well. Optical density (OD) measurements were performed at a wavelength of 570 nm using a 96-well plate reader (TECAN, Mannendorf, Switzerland), and a dose response curve was generated using SPSS software (Ichsyani et al.,2017). For the meassurement and evaluation of the effectivity of A. purpurata as the antidengue, the followings formula:

Selectivity Index of Extract ($SI_{extract}$) = CC_{50}/EC_{50}

In silico study

Hardware

Computational studies were conducted in silico using Dell Vostro 14 3000 hardware with an AMD Ryzen 5 3500U processor. The operating system running on the hardware was Windows 10 Ultimate 64-bit with Radeon Vega Mobile Gfx at 2.10 GHz.

Potential phytochemical compounds in A. purpurata for molecular docking experiment and ligand preparation

This work employed literature reviews to gather secondary data on phytochemical compounds in plants of the Alpinia genus in an attempt to identify particular chemicals with potential for use in molecular docking investigations. Scientific databases such as PubMed, ScienceDirect, and Google Scholar were investigated using the terms “Alpinia phytochemical compound,” “Secondary metabolites derived from Alpinia species,” and “Bioactive compounds in Alpinia species”. Experimental investigations reporting the identification or characterisation of secondary metabolite compounds from different Alpinia species were among the articles that fulfilled the inclusion criteria. A phytochemical profile that would represent the possible compounds in A. purpurata was then obtained by selecting, classifying, and descriptively analyzing the data based on the major compound groupings. Each specific compound that has been obtained and categorized based on the main compound group is then prepared to obtain several important data related to the formula, compound ID, canonical SMILES, and 3D structure. All of this data is obtained from the PubChem webserver (https://pubchem.ncbi.nlm.nih.gov/). The compound used as a test control for in silico is quercetin (CID: 5280343). The test ligands were prepared using Molecular Operating Environment (MOE) software (Chemical Computing Group, Montreal, Canada). The structures of the test compounds were directly inserted into the pharmacophore groups of the native ligands and then saved in mol2 format.

Drug-likeness screening and antiviral prospect of each identified metabolite

The drug-likeness capability of each previously identified test compound was screened using the SCFBio webserver (https://scfbio-iitd.res.in/software/drugdesign/lipinski.jsp) with guidelines from Lipinski's Rule of Five. Lipinski's Rule of Five sets rules for each compound to be classified as a drug, including molecular mass less than 500 Daltons, high lipophilicity (expressed as LogP less than 5), less than 5 hydrogen bond donors, less than 10 hydrogen bond acceptors, and molar refractivity should be between 40-130. Test compounds can proceed to further screening if they meet at least two of the total Lipinski Rule of Five (Lipinski, 2004). Furthermore, compounds that meet the Lipinski Rule of Five will be screened further using the PASS Online webserver (https://way2drug.com/PassOnline/). This screening is based on determining the specific ability of the compound as an antiviral by measuring the probable of active (Pa) and probable of inactive (Pi) values. Compounds can be categorized as having

antiviral activity if they have a Pa>Pi value. The three best compounds from the screening will be docked with the non-structural protein receptor from DENV-4.

Non-structural protein receptor preparation

Preparation of non-structural proteins using the Protein Data Bank webserver (https://www.rcsb.org/). In this study, three non-structural proteins essential for the dengue virus were used, which can aid the replication process and trigger an immune response. The three non-structural proteins are NS1 (PDB ID: 4AL8), NS3 helicase (PDB ID: 2JLQ), and NS5 (PDB ID: 4V0R) (Table 1). All receptor structures employed in this study were obtained from experimentally resolved DENV-4 proteins available in the Protein Data Bank. The selected structures corresponded specifically to DENV-4 non-structural proteins (NS1, NS3 helicase, and NS5), thereby ensuring biological relevance to the viral serotype investigated in the present study. The selected Before conducting the molecular docking experiment, the proteins were minimized and the root mean square deviation (RMSD) value was measured to determine protein stability using MOE software. Next, the test receptor was sterilized from water molecules and other contaminant ligands using PyMol v1.74 software (Schrödinger, LLC, USA) (Rahayu et al., 2025). To validate the reliability of the molecular docking protocol, redocking analysis was perfomed using the native ligands co-crystallized with each DENV-4 non-structural protein receptor. The native ligands were extracted from the receptor structures and subsequently re-docked into their original binding sites using the same docking parameters applied for the test compounds. The docking protocol was considered acceptable when the RMSD value between the experimentally determined native ligand conformation and the re-docked pose was below 2.0 Å, indicating reliable reproduction of the native binding orientation.

Table 1. Specific non-structural protein receptor of DENV-4 for docking target and validation of each Receptors through native ligand redocking.

Protein	Classification	PDB ID	RMSD of Native Ligand (Å)	Biological Function
NS1	Viral protein	4AL8	1.69	A non-enzymatic protein that is essential for replication complex formation and evasion of the host cell immune response
NS3 helicase	Hydrolase/RNA binding	2JLQ	1.56	A protein that functions as an enzyme to unwind double-stranded RNA structures during genome replication (RNA unwinding for viral replication).
NS5	Transferase	4V0R	1.18	The largest and most conserved non-structural protein, functioning in viral RNA replication (RdRp), RNA capping (methyltransferase), and evasion of the host immune system

Molecular docking experiment and complexes visualization

Molecular docking experiments of the test compounds against the NS1, NS3, and NS5 receptors were performed using MOE software. The test compounds were positioned at the active site of the protein, which had been minimized. The output generated from this molecular docking was a binding affinity score. The molecular docking method was validated by redocking the native ligand at the protein's active site. Visualization of the ligand-receptor complex was performed using BIOVIA Discovery Studio 2019 software (Dassault Systèmes, Vélizy-Villacoublay, France).

Molecular dynamics analysis

Molecular dynamics simulations were performed using the computer program AMBER 20. The associated protein or receptor and the ligand from the molecular modeling were separated from one another. After that, the protein was set up, the ligand was set up, and the protein-ligand complex was set up within the simulation box. The simulation box is filled with 26,375 TIP3P-type water molecules. The ff14SB force field is added to the complex to examine the forces, energy, and interactions between atoms within the complex. The complex is heated to a temperature of 310°K while keeping the number

of particles and the simulation volume constant. The system equilibration process is performed at constant pressure and temperature before proceeding to the trajectory generation phase.
Stereochemical quality analysis of protein structures using Ramachandran plot
Ramachandran plot analyasis was performed using the RamPlot webserver (https://ramplot.in/) to assess the stereochemical quality of the predictied protein structures. Protein models of NS1, NS3 helicase, and NS5 in PDB format were submitted to the server, and the backbone dihedral angles (φ and ψ) were analyzed. Residues were classified into favored, allowed, and disallowed regions across six residue categories (general residues, glycine, valine/isoleucine, pre-proline, trans-proline, and cis-proline). The proportion of residues located in favored regions was used as an indicator of structural reliability, whereas residues in disallowed regions were considered potential conformational outliners. Ramachandran plot distribution was further interpreted to evaluate secondary structural tendencies, including α-helix, β-sheets, and coil conformations (Kumar & Rathore, 2025).

ADME properties and toxicity analysis
Screening of pharmacokinetic parameters of test compounds with the best binding affinity values and potential as anti-dengue agents from molecular docking results was performed using the pkCSM webserver (https://biosig.lab.uq.edu.au/pkcsm/). The pkCSM webserver analyzes the ability of compounds based on their SMILES codes and their pharmacokinetic properties in the body. ADME consists of five major groups covering absorption, distribution, metabolism, and excretion of the compound. Each major group has its own specific sub-parameters used to measure the pharmacokinetic properties of compounds (Klimoszek et al., 2024). Furthermore, the specific toxicity of the selected test compounds is analyzed based on the structure of the pharmacophore group, fragments, and their similarity to other toxic compounds. This analysis was performed using the ProTox 3.0 webserver (https://tox.charite.de/protox3/). This was used to determine the acute toxicity (LD_{50}), hepatotoxicity, carcinogenicity, mutagenicity, immunogenicity, cytotoxicity, and organ-specific toxicities (Banerjee et al., 2024).

Data analysis
The mean ± standard deviation (SD) of triplicate measurements is used to represent all data. The half-maximal effective concentration (EC_{50}) and half-maximal cytotoxic concentration (CC_{50}) were estimated using non-linear regression in GraphPad Prism version 10.4.1 (San Diego, CA, USA). SI > 3 indicated selective antiviral activity (Ichsyani et al., 2017). The SI was computed as a ration of CC_{50}/EC_{50}.

Results

In vitro results
Antiviral testing on against DENV-4 showed that A. purpurata ethanol extract exhibited dose-dependent inhibitory acivity. The luminescence intensity decreased from 1.53×10^7 to 9.32×10^5 as the extract concentration increased from 50 to 150 µg/mL (Table 2). This decline indicates a reduction in viral replication activity in Vero E6 cells following extract treatment.
The EC_{50} value of the extract was 92.38 µg/mL, indicating its ability to inhibit 50% of viral replication. In addition, the percentage of cytopathic effect (%CPE) decreased from 78.82% at 50 µg/mL to 4.79% at 150 µg/mL, demonstrating a protective effect of the extract on infected cells (Figure 1).
Compared to the DENV control group (1.95×10^7 luminescence), all treatment groups showed markedly lower luminescence values, confirming the inhibitory activity of the extract on viral replication. The decrease in luminescence was proportional to the increase in the extract concentration, indicating a strong concentration-dependent antiviral effect.

Table 2. Antidengue replication assay results

Concentration of Alpinia purpurata extract (µg/ml)	**Luminescence**
50	1.53×10^7
100	9.62×10^6
150	9.31×10^5
Control DENV + Control Cell	1.95×10^7
Control Medium	5.83×10^2
EC_{50}	**92.38 µg/mL**

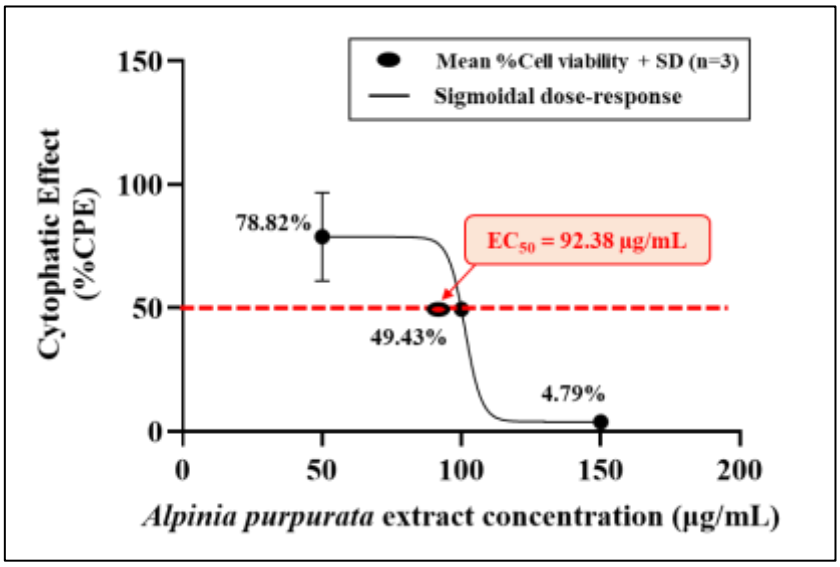

Figure 1. Dose-response relationship of Alpinia purpurata extract treatment against DENV-4. Bars = mean %CPE ± SD (n=3). Sigmoidal curve fitted using a three-parameter logistic (3PL) model. EC_{50} = 92.38µg/mL (as reported in the table 2).

The results of the study in Table 3 and Figure 2 show that the crude extract of A. purpurata is relatively safe (non-toxic) to Vero E6 cells. The CC_{50} value of 137.772 µg/mL is classified as low toxicity. This value is also higher than the EC_{50} value (100.923 µg/mL), which means that the extract still has the potential to be developed as a candidate antidengue agent.

Table 3. Antiviral activity of Alpinia purpurata treatment against DENV-2 measured by percentage of cell viability.

Concentration of Alpinia purpurata extract (µg/ml)	Mean Absorbance (OD) ± SD	%Cell viability ± SD
50	0,17 ± 0.003	111.44 ± 1.224
100	0,14 ± 0.001	83.03 ± 3.058
150	0,09 ± 0.018	38.65 ± 16.628
Cell Control	0,16 ± 0.002	100.00 ± 0.000
Medium Control	0,05 ± 0.001	0.00 ± 0.000
CC_{50}	-	**137.77 µg/mL**

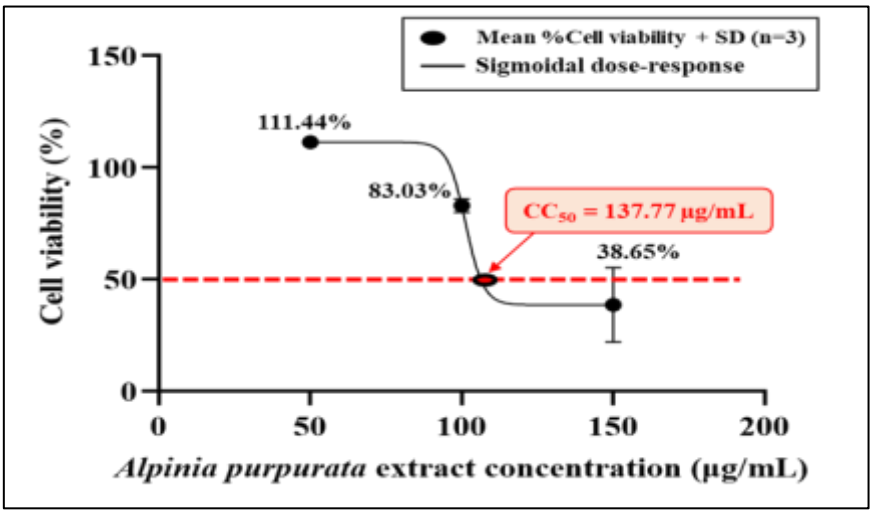

Figure 2. Dose-response relationship of Alpinia purpurata extract treatment against DENV-2. Bars = mean %Cell viability ± SD (n=3). Sigmoidal curve fitted using a three-parameter logistic (3PL) model. CC_{50} = 137.77 µg/mL (as reported in the table 3).

The potential anti-dengue implications of A. purpurata extract are illustrated by the CC_{50} value being greater than the EC_{50}. This indicates that the extract still shows relatively limited safety with regard to

its antiviral effects. Thus, crude A. purpurata extract can be considered as a candidate antidengue with low toxicity, although further optimization such as fractionation and purification of bioactive compounds is still needed to improve its effectiveness and efficiency, making it more ideal for use as a candidate antidengue drug.

Selectivity Index of Extract ($SI_{extract}$) = $\frac{CC50}{EC50} = \frac{137.77}{92.38}$ = 1,49

Potential phytochemical compounds in A. purpurata

Phytochemical analysis indicated that A. purpurata extract contains several groups of bioactive compounds, including terpenoids, phenylpropanoids, phenylalkanoids, flavonoids, and phenolic compounds (Table 4).

The terpenoid group includes compounds such as α-pinene and 1,8-cineole. Terpenoid identified in the extract are characterized by their isoprene-based backbone (C5 units) forming cyclic or bicyclic hydrocarbon structures, often with varying degrees of oxygenation.

The phenylpropanoid group is represented by (E)-methylcinnamate, possess a C6-C3 structural framework. This group consisting of an aromatic benzene ring attached to a three-carbon side chain.

Phenylalkanoids include shogaol and gingerol derivatives. This group compounds are structurally similar to phenylpropanoids but contain longer alkyl side chains linked to the aromatic ring, often with ketone or hydroxyl functional groups.

Flavonoids were identified as the dominant group in the group. These substances have the same C6-C3-C6 backbone structure, which is made up of two aromatic rings (A and B rings) joined by a heterocyclic pyran ring (C ring). Flavokawain B, pinostrobin, pinocembrin, kaempferol, galangin, kumatakenin, and pinobaksin-3-cinnamate are among the flavonoids found in the extract.

Gallic acid, ellagic acid, epicatechin, and 1'-acetoxychavicol acetate are among the phenolic chemicals found in the extract. The structural variety of this group of phenolic compounds is attributed to the presence of one or more hydroxyl groups that are directly connected to aromatic rings.

Table 4. Specific compounds identified in the extract based on previous literature studies

Compound	Formula	Class	References
α-pinene	$C_{10}H_{16}$	Terpenoid	Villaflores et al. (2010)
1,8-cineole	$C_{10}H_{18}O$	Terpenoid	
(E)-methylcinnamate	$C_{10}H_{10}O_2$	Phenylpropanoid	
4-shogaol	$C_{15}H_{20}O_3$	Phenylalkanoid	
6-shogaol	$C_{17}H_{24}O_3$	Phenylalkanoid	
10-shogaol	$C_{21}H_{32}O_3$	Phenylalkanoid	
6-gingerol	$C_{17}H_{26}O_4$	Phenylalkanoid	
8-gingerol	$C_{19}H_{30}O_4$	Phenylalkanoid	
10-gingerol	$C_{21}H_{34}O_4$	Phenylalkanoid	
Flavokawain B	$C_{17}H_{16}O_4$	Flavonoid	Mustahil et al. (2013)
Pinostrobin	$C_{16}H_{14}O_4$	Flavonoid	
Pinocembrin	$C_{15}H_{12}O_4$	Flavonoid	
Kaempferol	$C_{15}H_{10}O_6$	Flavonoid	Priyono et al. (2024)
Galangin	$C_{15}H_{10}O_5$	Flavonoid	
Kumatakenin	$C_{17}H_{14}O_6$	Flavonoid	Bian et al. (2014)
Pinobaksin-3-cinnamate	$C_{24}H_{18}O_6$	Flavonoid	
1'-acetoxychavicol acetate	$C_{13}H_{14}O_4$	Phenolic	Taib et al. (2020)
Gallic acid	$C_7H_6O_5$	Phenolic	Nampoothiri et al. (2015)
Ellagic acid	$C_{14}H_6O_8$	Phenolic	
Epicatechin	$C_{15}H_{14}O_6$	Phenolic	Cruz et al. (2023)

Screening of drug-likeness capability and antiviral prospect

Twenty phytochemical compounds from A. purpurata were screened, and all of them fulfilled at least two of Lipinski's Rule of Five criteria, suggesting that it has drug-like qualities. In comparison to the other compounds, a number of compounds, especially those from the phenolic group, such as gallic acid, ellagic acid, and epicatechin, showed higher Pa values (Table 5). This suggests that the stronger molecule with predicted antiviral activity was phenolic.

However, some compounds showed minor deviations from Lipinski parameters. Gallic acid exhibited lower molar refractivity, while epicatechin exceeded the recommended number of hydrogen bond donors.

Table 5. Specific compounds identified in the extract based on previous literature studies

Compound	Drug-likeness Parameters					Antiviral Potential	
	MW (g/mol)	LogP	HBD	HBA	MR	Pa	Pi
α-pinene	136.23	3.00	0	0	45.22	0.262	0.005
1,8-cineole	154.25	2.74	0	1	47.12	-	-
(E)-methylcinnamate	162.19	2.07	1	2	47.92	-	-
4-shogaol	248.32	3.26	1	3	73.30	0.267	0.050
6-shogaol	276.37	4.04	1	3	82.91	0.262	0.053
10-shogaol	332.48	5.60	1	3	102.14	0.262	0.053
6-gingerol	294.39	3.23	2	4	84.55	0.277	0.045
8-gingerol	322.44	4.01	2	4	94.16	0.277	0.045
10-gingerol	350.49	4.79	2	4	103.78	0.277	0.045
Flavokawain B	284.31	3.20	1	4	81.26	0.188	0.108
Pinostrobin	270.28	2.78	1	4	74.02	0.176	0.125
Pinocembrin	256.25	2.48	2	4	69.55	0.213	0.850
Kaempferol	286.24	2.28	4	6	76.01	0.260	0.054
Galangin	270.24	2.58	3	5	73.99	0.266	0.051
Kumatakenin	314.29	2.89	2	6	84.95	0.187	0.109
Pinobaksin-3-cinnamate	402.40	3.61	2	6	110.06	0.239	0.067
1'-acetoxychavicol acetate	234.25	2.08	0	4	62.95	0.165	0.141
Gallic acid	170.12	0.50	4	5	39.47	0.342	0.025
Ellagic acid	302.19	1.31	4	8	75.31	0.322	0.029
Epicatechin	290.27	1.22	5	6	74.33	0.378	0.017

MW, molecular weight; HBD, hydrogen bond donors; HBA, hydrogen bond acceptors; MR, molar refractivity; Pa, probable of active; Pi, probable of inactive; red shading, parameter didn't meet the Lipinski Rule of Five requirement (MW < 500 Dalton; HBD ≤ 5; HBA ≤ 10; LogP ≤ 5; MR 40-130); green shading, top three compound with highest antiviral potential. (-), no antiviral potential.

Molecular docking and complexes visualization results

The molecular docking analysis presented in Table 6 shows that among all candidate compounds identified from A. purpurata, three compounds, namely epicatechin, gallic acid, and ellagic acid, have higher Pa values than the others. In addition, the three compounds have the lowest binding energies to the DENV-4 non-structural proteins (NS1, NS3 helicase, and NS5 RNA polymerase). Among the three, epicatechin showed the highest binding affinity to NS1 (-4.27 kcal/mol), NS3 helicase (-7.00 kcal/mol), and NS5 (-6.14 kcal/mol), even surpassing the positive control quercetin on the NS3 protein type (-6.67 kcal/mol). These energy values indicate a stronger ligand-receptor complex stability, suggesting that epicatechin could act as a potential DENV-4 inhibitor. Epicatechin also showed higher affinity toward NS3 helicase compared to the control compound quercetin. The reliability of the docking protocol was confirmed through native ligand redocking analysis. The RMSD values obtained from the redocking procedure for each non-structural protein receptor were within the acceptable threshold (< 2.0 Å), demonstrating that the applied docking parameters were capable of reproducing the experimentally observed ligand binding orientation.

Table 6. Molecular docking and interactions result between receptor and test ligand

Compound	Receptor	Binding Affinity (kcal/mol)	Type of Interaction	Amino Acids Residue Involved
Epicatechin	NS1	-4.27	vdw	Gln39(H), Leu45(H), Gly42(H), Lys43(H)
			HI	Pro41(H)
			Amide-pi stacked	Arg40(H)

			π-sigma	Gly44(H)
	NS3 helicase	-7.00	vdw	Pro511(A), Glu514(A), Glu512(A), Pro319(A), Gly320(A), Trp488(A), Thr289(A), Met413(A), Asp409(A), Thr450(A), His485(A), Pro451(A), Lys480(A), Thr322(A)
			HI	Ala452(A)
			PHI	Glu512(A), Ser321(A), Lys515(A), Asp482(A)
			π-sigma	Ser453(A)
	NS5	-6.14	vdw	Lys61(A), Tyr103(A), Gly81(A), Thr104(A), Lys105(A), Val132(A), Phe133(A), Arg163(A), Glu111(A), Glu149(A), Gly148(A)
			HI	Ile147(A)
			PHI	Lys180(A), Asp146(A), Gly109(A), Asp131(A)
			π-π T-shaped	His110(A)
Gallic acid	NS1	-3.77	vdw	Leu45(H), Gly44(H), Arg40(H), Gly42(H)
			PHI	Lys43(H), Gln39(H), Pro41(H)
	NS3 helicase	-5.03	vdw	Ser321(A), Pro451(A), Thr450(A), Ser453(A), His287(A), Thr289(A), Trp488(A), Pro319(A), Glu512(A), Glu514(A), Lys480(A)
			HI	Ala452(A)
			PHI	Lys515(A), Gly320(A)
			π-anion	Asp482(A)
	NS5	-4.86	vdw	Val132(A), Phe133(A), Arg163(A), Lys105(A), Tyr103(A), Gly81(A), Gly83(A), Glu111(A)
			HI	Ile147(A)
			PHI	Asp131(A), Thr104(A), Lys130(A)
			π-π T-shaped	His110(A)
Ellagic acid	NS1	-4.21	vdw	Gly44(H), Leu45(H)
			HI	Pro41(H)
			PHI	Gln39(H), Gly42(H)
			π-lone pair	Lys43(H)
	NS3 helicase	-6.32	vdw	Thr322(A), Ser321(A), Ser453(A), Thr289(A), Phe288(A), Arg297(A), Trp488(A), Glu514(A), Pro511(A)
			HI	Pro319(A), Lys480(A)
			PHI	His287(A), Ala452(A), Pro451(A), Thr450(A), Gly320(A), Glu512(A), Lys515(A)
			π-anion	Asp482(A)

	NS5	-6.20	vdw	Cys82(A), Gly81(A), Glu149(A), Gly109(A), Gly148(A), Phe133(A), Val132(A)
			HI	Ile147(A)
			PHI	Asp131(A), Lys130(A), Gly83(A), Thr104(A), Glu111(A)
			π-π T-shaped	His110(A)
			Unfavorable donor-donor	Arg163(A)
Quercetin (control)	NS1	-4.37	vdw	Gln39(H), Arg40(H), Pro41(H), Gly44(H), Glu46(H)
			PHI	Leu45(H), Lys43(H)
	NS3 helicase	-6.67	vdw	Asp409(A), Met413(A), Trp488(A), Pro319(A), Glu512(A), Glu514(A), Pro511(A), Pro451(A), His485(A), Thr289(A)
			HI	Ala452(A)
			PHI	Thr450(A), Glu412(A), Lys480(A), His287(A), Lys515(A), Gly320(A)
			π-cation	Asp482(A)
			π-sigma	Ser453(A)
	NS5	-6.27	vdw	Gly109(A), Glu149(A), Phe133(A), Asp131(A), Val132(A), Tyr103(A), Gly83(A), Glu111(A)
			HI	Ile147(A)
			PHI	Lys130(A), Gly148(A), Arg163(A), Thr104(A), Gly81(A), Asp146(A), Lys180(A)
			π-π T-shaped	His110(A)

Van der Walls interaction; HI, hydrophobic interaction; PHI, hydrogen interaction; green shading, potential compound with highest binding affinity against each receptor; green shading, the best compound with the highest potential as antidengue for further analysis with ADME, toxicity, and visualization.

Further analysis through the interactions between the ligand and receptor complexes provided on Figure 3. In NS1, epicatechin formed hydrogen bonds with polar residues on the protein surface, alongside with Van der Walls and hydrophobic interactions that contributed to the overall binding stability.

In NS3 helicase, epicatechin formed hydrogen bond interactions with key residues, including Asp482 and surrounding amino acids within the ATP-binding site. The stability of the ligand-protein complex was enhanced by additional hydrophobic interactions with residues bordering the binding pocket.

Epicatechin engaged through polar and hydrogen bonding interactions with several residues in NS5, such as His110, Asp131, and Lys180. These connections were part of the NS5 RdRp active area, suggesting long-term binding within the catalytic pocket.

Furthermore, gallic acid and ellagic acid consistently bound to all target proteins. These compounds formed many hydrogen bonds with polar residues and pi-related (π) interactions with aromatic amino acids. Ellagic acid in particular showed notable hydrogen bonding networks due to its many hydroxyl groups, which increased its contact stability inside the binding sites. Additionally, π-π stacking and π-alkyl interactions with residues were made possible by the aromatic ring topologies of these compounds. Alkyl interactions with binding pocket residues further stabilize the ligand-protein complexes.

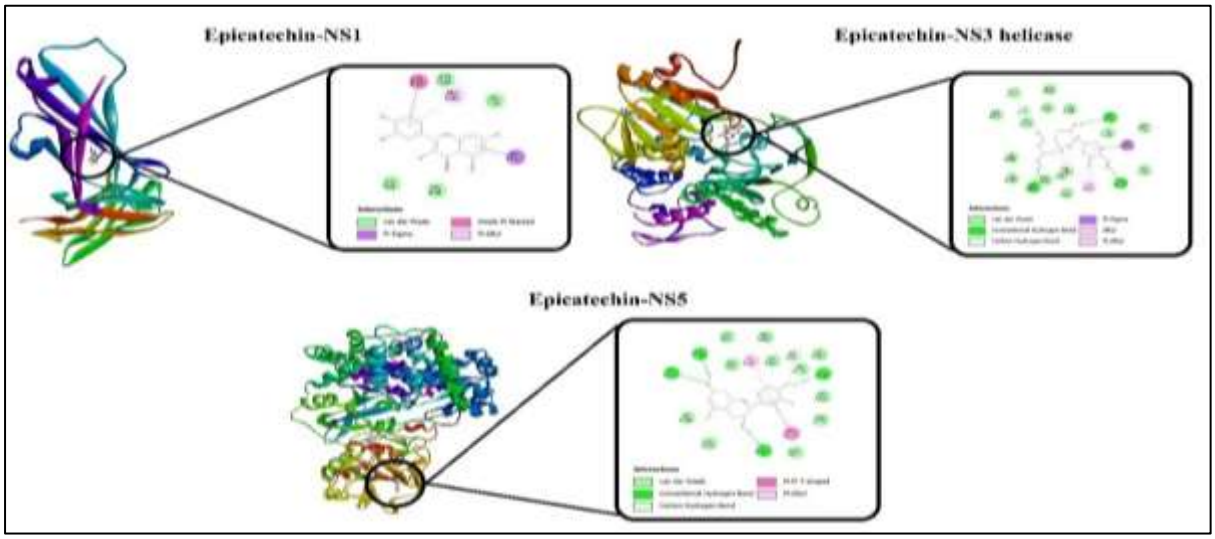

Figure 3. Visualization of chemical interaction between non-structural protein receptors and epicatechin.

Molecular dynamics simulation assessment results

The stability of the complexes formed by epicatechin and the NS1, NS3, and NS5 receptors was examined using molecular dynamics simulations. The stability of the complex and the changes in the protein amino acids during complex formation were evaluated using the root mean square deviation (RMSD) and root mean square fluctuation (RMSF) metrics. The binding energy required to maintain the complex's stability was also examined using the MM-PBSA parameter.

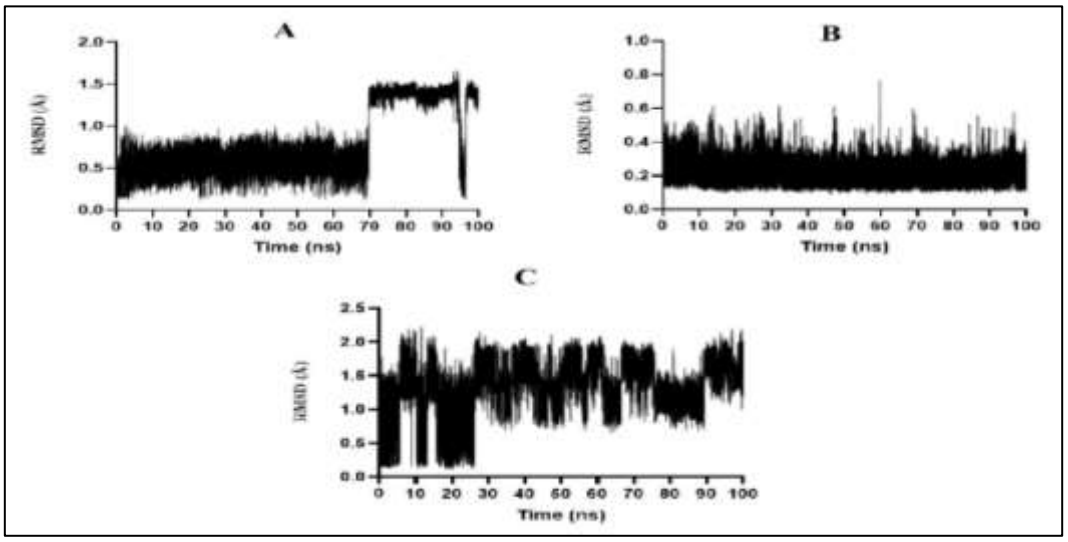

Figure 4. Root Mean Square Deviation (RMSD) plots for the ligand in molecular dynamics simulations of the epicatechin complex with the NS1 (A), NS3 helicase (B), and NS5 (C) receptors.

RMSD analysis of the ligand in the epicatechin complex with the NS1, NS3, and NS5 receptor targets was performed over 100 ns to assess ligand stability within the complex during molecular dynamics simulations (Fig. 4A–C). The epicatechin complex with the NS1 receptor exhibited stable fluctuations during the 0–70 ns time window, with an RMSD range of 0.1–1.0 Å. Subsequently, the RMSD value became unstable, increasing to 1.5 Å between 70–90 ns, followed by a decrease to 0.2 Å by 95 ns, and a subsequent rise back to 1.5 Å between 95–100 ns (Fig. 4A). The RMSD profile for the epicatechin complex with the NS3 helicase receptor shows high fluctuations at several time points. At time 60, the RMSD value reached 0.8 Å (Fig. 4B). In the epicatechin-NS5 receptor complex, the RMSD profile showed unstable fluctuations and did not reach a plateau during the simulation process, but the RMSD value remained below 2.0 Å (Fig. 4C).

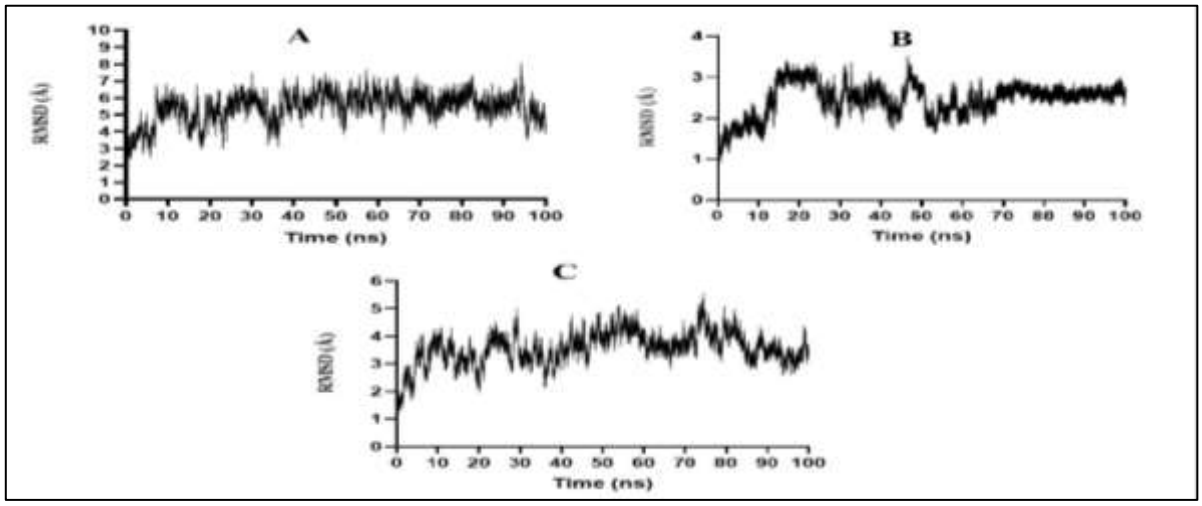

Figure 5. Root Mean Square Deviation (RMSD) plots for the molecular dynamics simulations of the epicatechin complex with the NS1 (A), NS3 helicase (B), and NS5 (C) receptors.

The analysis of protein RMSD aims to assess the stability of the protein within its complex with the ligand during the simulation process. In the epicatechin-NS1 receptor complex, the RMSD profile reached equilibrium between 40 and 95 ns, with RMSD values ranging from 5.0 to 6.0 Å (Fig. 5A). In the complex with the NS3 helicase receptor, the RMSD profile shows a plateau at 15–25 ns with an RMSD of approximately 3.0 Å and at 70–100 ns with an RMSD of about 2.5 Å (Fig. 5B). The RMSD profile for the epicatechin-NS5 receptor complex exhibits unstable fluctuations and only reaches a plateau at 60–70 ns with an RMSD of approximately 3.5 Å (Fig. 5C).

RMSD analysis demonstrated that the ligand-protein complexes generally maintained structural stability throughout the simulation period. However, moderate fluctuations were observed, particularly in the NS1 and NS5 complexes. These variations may reflect local conformational adjustment of the protein-ligand systems during dynamics equilibration rather than complete destabilization of the complexes. Compared with the apo protein, the ligand-bond systems exhibited comparable or improved structural behavior, suggesting that the interactions were maintained during the simulation.

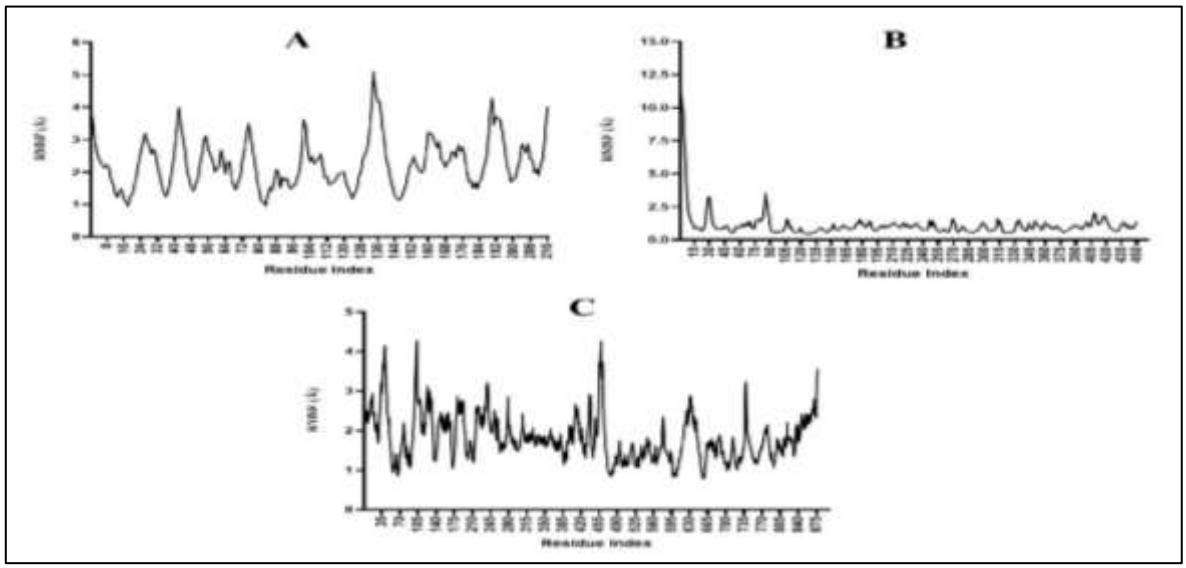

Figure 6. Root Mean Square Fluctuation (RMSF) plots of amino acid residues from molecular dynamics simulations of the epicatechin complex with the NS1 (A), NS3 helicase (B), and NS5 (C) receptors.

RMSF analysis of amino acid residues aims to assess the flexibility of amino acid residues after a ligand binds to a protein (Alsaady et al., 2026). In the epicatechin-NS1 receptor complex, the RMSF profile shows relatively high fluctuations across all amino acid residues, with RMSF values ranging from 1.0 to 4.0 Å. The RMSF profile exhibits the highest fluctuations, with an RMSF value reaching 5.0 Å at residue index 136 (Fig. 6A). The RMSF profile of the epicatechin-NS3 helicase receptor complex shows RMSF values below 2.5 Å across the residue index range of 105–450 and does not exhibit significant

fluctuations. At around residue index 30 and in the residue index range of 75–90, there are significant fluctuations with RMSF values exceeding 2.5 Å (Fig. 6B). The profile of the complex with the NS5 receptor also shows the same pattern, with several amino acid residues exhibiting relatively high fluctuations. In the residue indices 315–385, a plateau condition is reached with an RMSF value of approximately 2.0 Å, and the residue indices 490–560 have a lower RMSF value of 1.5 Å. Several amino acid residue indices show the highest fluctuations with RMSF values reaching 4.0 Å (Fig. 6C).

Table 7. The binding value of the epicatechin complex with the NS1, NS3, and NS5 receptors.

Complexes	ΔGgas	ΔGsolv	ΔGtotal (ΔGgas + ΔGsolv)
EP-NS1	-251.198	238.084	-13.114
EP-NS3	-269.389	248.363	-30.658
EP-NS5	-9.055	6.438	-2.616

The Molecular Mechanics Poisson-Boltzmann Surface Area (MM/PBSA) parameter is used to analyze the free energy required to form ligand-receptor complexes in molecular dynamics simulations. This parameter is also capable of evaluating the most reliable modes of ligand-receptor interaction (Tuccinardi, 2021). Based on Table 7, the epicatechin-NS3 complex has the lowest total free energy (Gtotal = -21.0256 kcal/mol) compared to the other complexes. Meanwhile, the epicatechin-NS5 complex has the highest total free energy (Gtotal = -2.6165 kcal/mol).

Stereochemical quality of protein structures results

The stereochemical quality of the protein structure models was evaluated using a Ramachandran plot via the RamPlot web server, which assesses the distribution of protein backbone dihedral angles (φ and ψ) to determine whether the conformations of amino acid residues align with acceptable protein stereochemical parameters. Based on the analysis results, the three target proteins exhibited excellent geometric quality, as the majority of residues were located in the favoured region, which serves as the primary indicator of protein structural validity (Figure 7).

The NS1 protein showed that 98.252% of residues were in the favored region, 1.748% in the allowed region, and no residues were found in the disallowed region. The NS1 model is very dependable for use in additional structural analysis since its distribution shows that almost all protein backbone residues are in the most stereochemically stable conformations. The lack of leftovers in the dissalowed area suggests that the structural model has no appreciable local distortions.

The NS3 helicase protein shows similar results with 97.773% of residues in the favoured region, 2.227% in the allowed region, and 0% in the disallowed region. These values indicate that the backbone structure of the helicase domain has a highly stable conformation and aligns with the structural characteristics of functional proteins. The dominance of residues in the favoured region is crucial because the helicase domain requires conservation of the backbone geometry to maintain its biological activity, particularly in the mechanisms of nucleotide binding and viral RNA processing.

In the NS5 protein, 96.809% of the residues are located in the favored region, 2.955% in the allowed region, and only 0.236% in the disallowed region. Although there is a small number of residues in the disallowed region, this percentage remains very low and generally falls within acceptable limits for a predicted protein structure model.

Overall, all three protein models meet excellent stereochemical quality criteria, as they have more than 96% of residues in the favoured region. This indicates that the structural models have been assembled into a backbone conformation that closely resembles the natural protein structure.

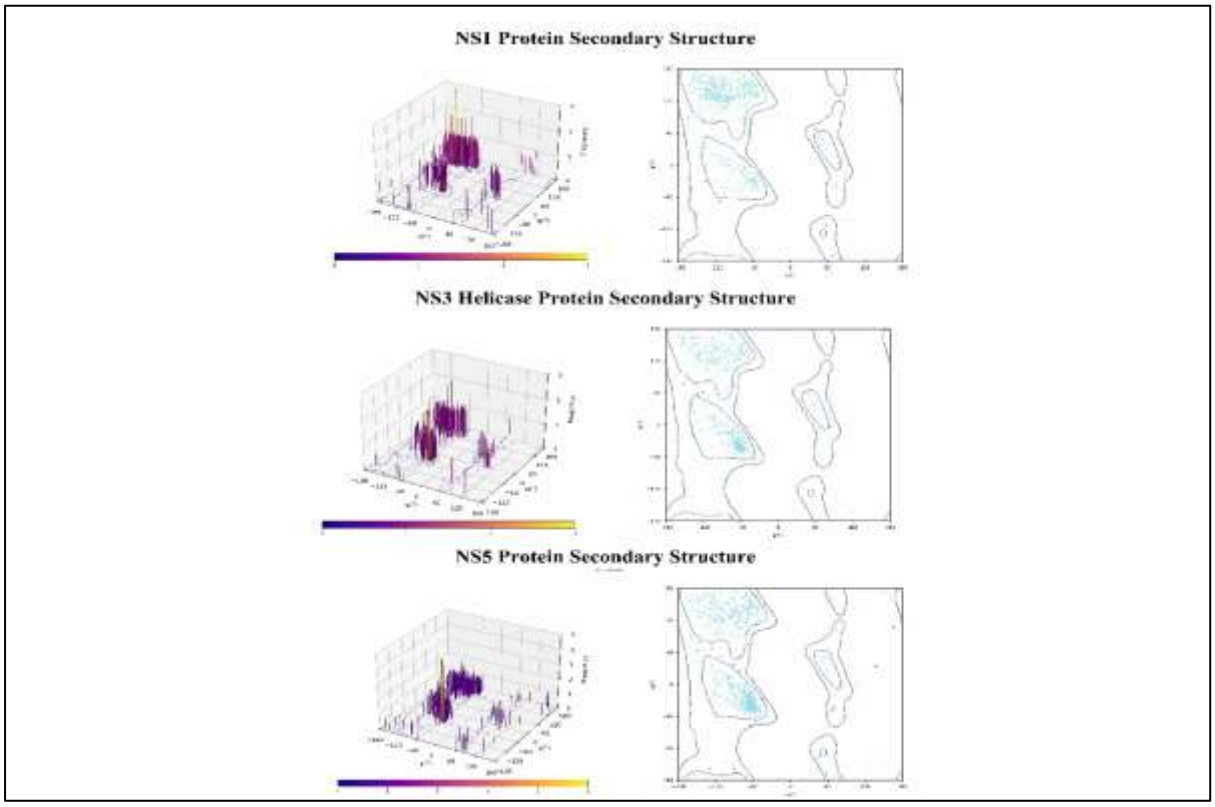

Figure 7. Stereochemical quality of protein structures result (NS1 (98.252% favoured; 1.748% allowed; 0% dissalowed), NS3 helicase (97.773% favoured; 2.227% allowed; 0% dissalowed), and NS5 (96.809% favoured; 2.955% allowed; 0.236% dissalowed)

ADME properties and toxicity analysis results

ADME analysis of epicatechin showed favorable pharmacokinetic properties (Table 8). The compound demonstrated good intestinal absorption (68.829%) and moderate distribution (VDss: 1.027 logL/kg). In terms of activity-related parameters, epicatechin show consistent performance, as indicated by their favorable values. This compound tends to display stronger interaction profiles and more stable characteristics relative to the remaining phytochemicals.

From pharmacokinetic perspective, epicatechin demonstrated suitable absorption characteristics, with a good intestinal absorption and moderate distribution properties. The compound showed low permeability across blood-brain barrier (BBB) and central nervous system (CNS), indicating limited distribution to brain tissues.

In the term of metabolism, epicatechin was not predicted to act as a substrate or inhibitor of major cytochrome P450 enzymes, suggesting a low potential for metabolic interactions. The compound also exhibited moderate clearance and showed no interaction with renal OCT2 transporters.

Table 8. ADME properties screening results of epicatechin

Type	Parameter	Epicatechin	Unit
Absorption	Water solubility	-3.117	Numeric (log mol/L)
	Caco2 permeability	-0.283	Numeric (log Papp in 10^{-6} cm/s)
	Intestinal absorption (human)	68.829	Numeric (% Absorbed)
	Skin Permeability	-2.735	Numeric (log Kp)
	P-glycoprotein substrate	Yes	Categorical (Yes/No)

	P-glycoprotein I inhibitor	No	Categorical (Yes/No)
	P-glycoprotein II inhibitor	No	Categorical (Yes/No)
Distribution	VDss (human)	1.027	Numeric (log L/kg)
	Fraction unbound (human)	0.235	Numeric (Fu)
	BBB permeability	-1.054	Numeric (log BB)
	CNS permeability	-3.298	Numeric (log PS)
Metabolism	CYP2D6 substrate	No	Categorical (Yes/No)
	CYP3A4 substrate	No	Categorical (Yes/No)
	CYP1A2 inhibitior	No	Categorical (Yes/No)
	CYP2C19 inhibitior	No	Categorical (Yes/No)
	CYP2C9 inhibitior	No	Categorical (Yes/No)
	CYP2D6 inhibitior	No	Categorical (Yes/No)
	CYP3A4 inhibitior	No	Categorical (Yes/No)
Excretion	Total Clearance	0.183	Numeric (log ml/min/kg)
	Renal OCT2 substrate	No	Categorical (Yes/No)

Figure 8 presents the predicted profile of epicatechin across multiple toxicity endpoints. Epicatechin exhibited predicted LD_{50} value of 10,000mg/kg, which classifies it into toxicity class 6, indicating non-toxic or safe category. This high LD_{50} value reflects low acute toxicity following oral exposure.

Across several toxicity endpoints, epicatechin was predicted to be non-toxic. These include immunotoxicity, neurotoxicity, cytotoxicity, hepatotoxicity, ecotoxicity, carcinogenicity, and mutagenicity, indicating the absence of major toxicity risks in these categories.

However, epicatechin showed potential toxicity signals in specific endpoints. Nutritoxicity and nephrotoxicity were predicted for these substances, indicating potential impacts on kidney function and metabolic processes. Furthermore, epicatechin showed a positive prediction for respiratory toxicity, which was found to be the most noticeable toxicity signal out of all the measures that were assessed.

Overall, the toxicity profile depicted in Figure 8 shows that epicatechin is essentially non-toxic in the majority of biological systems, with only minor hazards associated with nephrotoxicity, respiratory toxicity, and nutritoxicity in the cells.

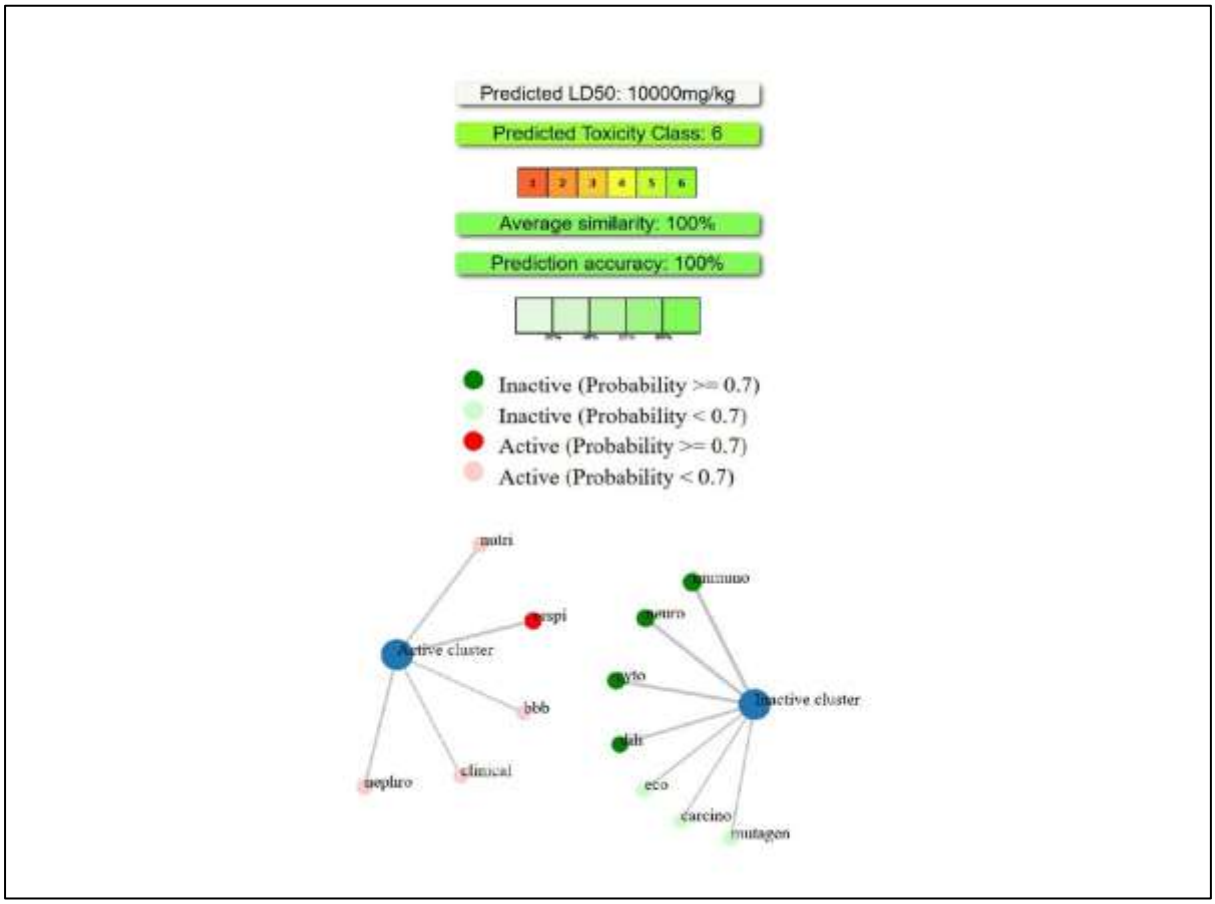

Figure 8. Toxicity assay prediction of epicatechin

Discussion

The current study demonstrates that A. purpurata extract has moderate but considerable antiviral activity against DENV-4 based on both in vitro and in silico data. The determined EC_{50} value of 92.38 µg/mL indicates that the extract can suppress replication at a identifiable level, as is characteristic of crude extracts containing complex combinations of bioactive compounds. Plant-derived antivirals with EC_{50} values between 20 and 100 µg/mL are often classified as having moderate activity when compared to isolated compound with more specific molecular targets (Owen et al., 2022).

The extract showed a cytoprotective function in infected Vero E6 cells by considerably lessening its cytopathic effects relative to its antiviral action. This combined activity suggests that the extract preserves the integrity of host cells in addition to preventing viral reproduction. These effects are often associated with the presence of several secondary metabolites acting in concert rather than a single dominant molecule.

The increase in cell viability at low concentrations (50 µg/mL) is thought to be related to the presence of flavonoid and terpenoid secondary metabolites in A. purpurata. These compounds have previously been known to act as antioxidants that can protect cells from oxidative stress caused by viral infections. Compounds such as quercetin, β-pinene, and galangin have also been reported to have cytoprotective activity and are able to modulate cellular signaling pathways to increase cell proliferation (Aladaileh et al., 2019).

The effectiveness and safety of an antiviral drug are assessed using the SI values. A high SI value indicates that the extract effectively suppresses viral replication with minimal toxic effects on host cells. Based on the SI categories, an SI value below 5 is classified as weak. This means that the extract still possesses antiviral activity, but its inhibition of DENV proteins is not yet strong enough to significantly weaken the dengue virus. By comparison, other natural extracts such as Curcuma longa exhibit an SI value of 4.8 against DENV-2, which is considered sufficiently good for the early stages of natural antiviral development (Ichsyani et al., 2017). Thus, the SI values < 2 obtained by the extract and the control drug are still relatively low and indicate that both possess potential antiviral activity; however, they are not yet safe enough for direct application without further modification. Further steps, such as fractionation, can be undertaken to isolate specific active compounds within the A. purpurata extract.

One of the compounds identified in this study is epicatechin from the flavonoid group, which, in the in silico simulations, exhibits a higher binding energy value compared to the control.
At higher concentrations (150 μg/mL), the extract significantly reduced cell viability (38.39%). This is likely due to the pro-oxidative effects of some phenolic compounds at higher concentrations. The emergence of excessive pro-oxidative effects can trigger apoptosis and cell membrane dysfunction. MTT measures the reduction of tetrazolium by mitochondrial dehydrogenase. Antioxidants from certain phytochemicals can increase signals at low doses (cytoprotective effect) and then decrease them at high doses (pro-oxidative), explaining the pattern of cell viability decline from 111% to 38%.
Terpenoids, phenylpropanoids, phenylalkanoids, flavonoids, and phenolic compounds are among the many bioactive substances found in A. purpurata, based on phytochemical study. A multitarget antiviral mechanism is supported by this variety. In the early stages of infection, 1,8-cineole can improve host antiviral responses by suppressing NF-κB pathways and modifying interferon signaling (Yang et al., 2020).
By focusing on the host mechanism and viral reproduction activites, phenylalkanoid substances as shogaol and gingerol further contribute. By supressing NS5 RdRp activity and lowering pro-inflammatory cytokine production, these compounds have been shown to limit both viral replication and host tissue damage (Jiménez De Oya et al., 2019).
From all the compounds discovered, flavonoid and phenolics appear to be essential for antiviral activity. Important viral proteins including NS3 helicase and NS5 are known to interact with kaempferol, galangin, and pinocembrin from the flavonoid group by stabilizing inactive viral enzyme conformations and preventing replication (Nie et al., 2021). Furthermore, by focusing on envelope proteins and blocking membrane fusion, certain flavonoids can stop viruses from entering the cells.
Through both direct and indirect mechanism, phenolic substances such as gallic acid, ellagic acid, and epicatechin can also increase antiviral activity potential. By using their antioxidant activity, these substances can influence cellular responses and inhibit viral replication proteins. Futhermore, by lowering reactive oxygen species (ROS) and neutralizing acidic intracellular vesicles necessary for viral maturation, phenolics can produce non-infectious viral particles (Jung et al., 2019). By inhiniting inflammatory pathways and boosting type I interferon responses, they also support antiviral immunity.
Epicatechin, gallic acid, and ellagic acid from phenolic class were found to be the most promising candidates in drug-likeness and antiviral prediction tests. Based on their structure, these compounds showed high expected antiviral activity, which is in line with earlier research showing phenolics are potent inhibitors of dengue virus enzymes like helicase and protease (Dwivedi et al., 2020). The high hydrogen bond donor counts of epicatechin and the low molar refractivity of galic acid represent two examples of deviations from Lipinski's Rule of Five that may improve binding interactions with viral targets rather than limit activity. Curcumin, which preserves its efficacy via an allosteric inhibitory mechanism, has shown similar fluctuations (Lim et al., 2020).
Further understanding of the atomic-level mechanism of action was obtained by molecular docking research. All three target proteins (NS1, NS3 helicase, and NS5) demonstrated the strongest and most reliable binding affinity for epicatechin among the substances being studied. RNA unwinding, a crucial stage in viral replication, may be prevented by its interaction with important residues Asp482 in the ATP-binding site of NS3 helicase (Halim et al., 2017). Furthermore, interactions with the NS5 residues His110, Asp131, and Lys180 suggest that RNA production may be inhibited.
Since it enables epicatechin to disrupt numerous stages of the viral replication cycle, this dual-target inhibitory strategy is especially significant. Phenolic compounds from Theobroma cacao have been shown to exhibit similar multitarget activity and to firmly inhibit NS5 RdRp using in silico approaches (Huq et al., 2024).
Furthermore, persistent interactions between ellagic acid and gallic acid were discovered, particularly in allosteric regions. According to this mechanism, they may prevent replication complexes and protein dimerization from forming. Aromatic rings are known to facilitate enzyme inhibition through π-interactions with important residues. Strong correlations between flavonoid structures and dengue protease complex inhibition have been found in structure-activity link investigations, supporting this conclusion (Sarwar et al., 2018).
The stability and strength of epicatechin's interaction with the DENV-4 target proteins are further demonstrated by the outcomes of the molecular dynamic simulation (Figure 4-6) and the energy statistics in Table 7. The RMSD profiles demonstrate that the protein-ligand complexes retain structural stability across the simulation period, with comparatively small fluctuations typically associated with conformational adjustment toward equilibrium states. Similarly, RMSF analysis reveals restricted flexibility in the majority of residues, with bigger changes mostly seen in loop areas, indicating that epicatechin binding does not significantly cause structural instability. Additionally, the binding free

energy values in Table 7 indicate favorable interaction energies that promote the formation of stable complexes between the target proteins and epicatechin. These findings are consistent with previous studies showing that constant RMSD and low residue fluctuation suggest strong and stable ligand-protein interactions (Hollingsworth & Dror, 2018). It's well known that favorable binding free energy is a crucial marker of both spontaneous and long-term molecular interactions in protein-ligand systems. Although molecular dynamics simulations supported the stability of the ligand-protein interactions, the observed RMSD and RMSF fluctuations, particularly within the NS1 and NS5 complexes, indicate the presence of dynamic conformational changes during the simulation. Such fluctuations are commonly observed in protein-ligand systems due to intrinsic flexibility of protein regions and ligand-induced conformational adaptation. Therefore, the MD findings should be interpreted as evidence of maintained interaction stability under dynamic conditions rather than absolute structural rigidity. Further experimental validation is required to confirm the biological relevance of these computational predictions.

The precision of these docking results is further supported by the high stereochemical quality of the protein structures used in this study. Over 96% of residues in all protein models were found in favored regions, according to Ramachandran plot analysis (Fernández-Quintero et al., 2023). According to Pražnikar et al. (2019), small changes found in specific regions are probably related to flexible loop structures and have no effect on the overall stability of the protein.

ADME analysis showed a positive pharmacokinetic profile. The drug exhibited a moderate capacity to penetrate the central nervous system, a modest tissue distribution, and good intestine absorption, all of which may lower the risk of neurotoxicity. A low likelihood of drug-drug interactions, a crucial problem in antiviral therapy, is suggested by the lack of notable interactions with cytochrome P450 enzymes (Borges et al., 2018).

Although the ADME analysis suggested favorable pharmacokinetic characteristics for epicatechin, these findings should be interpreted with caution because they are based exclusively on computational prediction models. In silico ADME tools provide valuable preliminary insights into absorption, distribution, metabolism, and excretion profiles. However, it cannot fully capture the complexity of biological systems and interindividuality variability. Consequently, the predicted pharmacokinetic properties require further validation through experimental approaches, including in vitro absorption and metabolism studies as well as in vivo pharmacokinetic investigations. Therefore, the present ADME results should be regarded as supportive evidence for compound prioritization rather than definitve confirmation of pharmacokinetic behavior.

Additional proof of epicatechin's safety includes its lack of immunotoxicity, neurotoxicity, cytotoxicity, hepatotoxicity, ecotoxicity, carcinogenicity, and mutagenicity effects. These findings are consistent with previous studies demonstrating its safety in biological systems (Alkinani et al., 2021). However, the expected respiratory toxicity signal indicates that more in vivo studies are needed for validation.

Although the overall toxicity prediction suggested a favorable safety profile for epicatechin, several potential adverse effects, including predicted respiratory toxicity, nephrotoxicity, and nutritoxicity, warrant careful consideration. These predicted toxicological endpoints do not necessarily indicate clinically relevant toxicity but rather represent computational signals that may require further investigation. Such predictions are generated based on structural similarity and machine-learning models and may not fully reflect biological responses under physiological conditions. Nevertheless, these findings highlight the importance of condicting experimental toxicological evaluations, including cellular toxicity assays and animal studies, to verify the safety profile of epicatechin and determine whether these predicted effects have biological significance.

The overall findings of the study show that A. purpurata has the potential to be a natural antiviral agent against DENV-4. Because of its superior pharmacokinetic properties, multitarget molecular interactions, and in vitro antiviral activity, its bioactive components, especially epicatechin, may be promising candidates for new therapeutic development. The combinatoral effects of many phytochemicals that target different stages of the viral life cycle provide significant evidence for the development of plant-based antidengue therapies.

This study highlights the potential of A. purpurata as a source of antidengue agents through an integrated approach that combines phytochemical profiling from previous literature studies, in vitro antiviral activity, and computational analyses using molecular docking, molecular dynamics, ADME, and toxicity analysis. The primary discovery is that epicatechin is a promising multitarget ligand, as demonstrated by its consistent binding across NS1, NS3 helicase, and NS5, as well as its outstanding pharmacokinetic and toxicological profile. The results also point to a multitarget and multicomponent approach where different phytochemical classes may cooperate to block different stages of the dengue

virus life cycle. These findings are significant because they offer an alternative method for developing antivirals, particularly in due to the lack of effective and safe dengue treatments.
Despite these promising findings, this study has several limitations. The antiviral activity was evaluated in vitro and computational predictions, which may not fully reflect in vivo physiological conditions. Furthermore, pharmacokinetic and toxicity profiles were relied on in silico models, requiring additional experimental validation. In order to validate multitarget interactions, future research should concentrate on the in vivo assessment, isolation, and characterisation of active molecules as well as comprehensive mechanistic investigations. To assist the development of molecules derived from A. purpurata as possible antidengue therapies, more research into formulation techniques and dose optimization is also required. Another limitation of this study is that phytochemical constituents used for computational analyses were selected based on previously published reports of A. purpurata rather than direct chemical characterization of the extract used in the present study. Consequently, batch-specific variations in phytochemical composition could not be assessed. Future studies should incorporate analytical characterization techniques, such as LC-MS/MS or GC-MS, to standardize the extract and confirm the presence and abundance of the proposed bioactive compounds.

Conclusions

This study shows that Alpinia purpurata ethanol extract has modest but significant antiviral activity against DENV-4, as shown by a significant decrease in cytopathic effects in infected Vero E6 cells and dose-dependent inhibition of viral replication with an EC_{50} value of 92.38 µg/mL. Cytotoxicity evaluation using the MTT assay revealed a CC_{50} value of 137.77 µg/mL and SI of 1.49, indicating measurable antiviral activity with limited selectivity in its crude extract form. The extract also significantly reduced cytopathic effects in infected Vero E6 cells. Through strong and reliable binding to important non-structural proteins NS1 (-4.27 kcal/mol), NS3 helicase (-7.00 kcal/mol), and NS5 (-6.14 kcal/mol), integrated in silico study demonstrated that phenolic chemicals, especially epicatechin, play a crucial role in this activity. This mechanism suggests an inhibitory multitarget mechanism. Molecular dynamics simulations, supported by favorable binding free energy profiles, further confirmed the stability of the ligand-protein complexes, especially for NS3 helicase. Furthermore, based on ADME and toxicity projections, epicatechin showed promising pharmacokinetic properties and a generally safe toxicity profile, supporting its potential as a lead chemical for antiviral research. In silico ADME and toxicity assessments suggested favorable pharmacokinetic characteristics and a low predicted toxicity profile for epicatechin. Nevertheless, these computational predictions require experimental validation before definitive conclusions regarding its pharmacological suitability can be established. The combination of in vitro validation and computation insight highlights a synergistic, multi-compound and multitarget mode of action derived from A. purpurata phytochemicals. Overall, this study provides novel evidence supporting A. purpurata as a potential source of anti-DENV-4 agents and identifies epicatechin as a promising multitarget inhibitor of viral replication. These findings offer a valuable foundation for further in vivo validation, compound isolation, and the development of plant-based antiviral therapeutics targeting dengue virus.

Conflict of Interest
The authors declare that no conflict of interests.

Author Contributions
Conceptualization: MAH, MRT, WDM, DWN; design and material: MAH, WDM, DWN, RAD, PAI; supervision and resources: WDM, DWN, RAD; data collection and literature research: MAH, AUR; analysis and interpretation: MAH, TW; writing manuscript: MAH, MRT, WDM, DWN, AUR; critical review: RAD.

Data Availability Statement
All data supporting the findings of the study are available within the manuscript.

Funding and Acknowledgments
This study was supported by Program Magister Menuju Doktor untuk Sarjana Unggul (PMDSU) Scholarship scheme with Contract Number 067/C3/DT.05.00/PL-MULTITAHUNLANJUTAN/2026 and Specific Contract Number 1115/B/DST/UN3.DRI/PT.01.03/2026 from the Ministry of Higher Education, Research, and Technology, Republic of Indonesia. The authors would like to express thank

you for the Dengue Laboratory, Institute of Tropical Diseases, Universitas Airlangga for providing the materials regarding to this dengue research.

Informed Consent Statement
Not applicable.

Abbreviations
ADE, antibody-dependent enhancement; ADME, absorption, distribution, metabolism, excretion; CAT, catalase; CPE, cytopathic effects; DENV, dengue virus; DHF, dengue hemorrhagic fever; NS, non-structural protein virus; RMSD, root mean square deviation; RMSF, root mean square fluctuation; RNA, ribonucleic acid; SI, selectivity index; SOD, superoxide dismutase.

References

1. Aladaileh, S. H., Abukhalil, M. H., Saghir, S. A. M., Hanieh, H., Alfwuaires, M. A., Almaiman, A. A., Bin-Jumah, M., Mahmoud, A. M. (2019). Galangin activates Nrf2 signaling and attenuates oxidative damage, inflammation, and apoptosis in a rat model of cyclophosphamide-induced hepatotoxicity. Biomolecules, 9(8), 346. https://doi.org/10.3390/biom9080346
2. Alkinani, K. B., Ali, E. M. M., Al-Shaikh, T. M., Awlia Khan, J. A., Al-Naomasi, T. M., Ali, S. S., Abduljawad, A. A., Mosa, O. F., & Zafar, T. A. (2021). Hepatoprotective effects of (-) epicatechin in CCl_4-induced toxicity model are mediated via modulation of oxidative stress markers in rats. Evidence-based Complementary and Alternative Medicine: eCAM, 2021, 4655150. https://doi.org/10.1155/2021/4655150
3. Alsaady, I. M., Gattan, H. S., Aljahdali, S. M., Alruhaili, M. H., Dwivedi, V. D., & Azhar, E. I. (2026). Conformational dynamics and binding free energy analyses unveil a stable flavonoid inhibitor of dengue virus NS5 polymerase. Scientific Reports, 16, 7761. https://doi.org/10.1038/s41598-026-38864-2
4. Bharadwaj, S., Lee, K. E., Dwivedi, V. D., Yadava, U., Panwar, A., Lucas, S. J., Pandey, A., & Kang, S. G. (2019). Discovery of Ganoderma lucidum triterpenoids as potential inhibitors against Dengue virus NS2B-NS3 protease. Scientific Reports. 9(1), 19059. https://doi.org/10.1038/s41598-019-55723-5
5. Bian, M., Wang, H., Kang, J., Chen, R., Yang, Y., Wu, H. (2014). Flavonoids from the seeds of Alpinia galanga Willd. Yaoxue Xuebao, 49(3), 359-362.
6. Banerjee, P., Kemmler, E., Dunkel, M., Preissner, R. (2024). ProTox 3.0: A webserver for the prediction of toxicity of chemicals. Nucleic Acids Research, 52(W1), W513–W520. https://doi.org/10.1093/nar/gkae303
7. Borges, G., Ottaviani, J. I., van der Hooft, J. J. J., Schroeter, H., & Crozier, A. (2018). Absorption, metabolism, distribution and excretion of (-)-epicatechin: A review of recent findings. Molecular Aspects of Medicine, 61, 18–30. https://doi.org/10.1016/j.mam.2017.11.002
8. Cheng, Y., Sheen, J., Hu, W. L., Hung, Y. (2017). Polyphenols and oxidative stress in atherosclerosis-related ischemic heart disease and stroke. Oxidative Medicine and Cellular Longevity, 1, 8526438. https://doi.org/10.1155/2017/8526438.
9. Cruz, J. D., Mpalantinos, M. A., Oliveira, L. R., Branches, T. G., Xavier, A., Souza, F. C. A., Agyuar, J. P. L., Ferreira, J. L. P., Silva, J. R. A., Amaral, A. C. F. (2023). Nutritional and chemical composition of Alpinia zerumbet leaves, a traditional functional food. Food Research International, 113, 113517.
10.Culbertson, A.T., Liao, M. (2025). Cryo-EM of human P-glycoprotein reveals an intermediate occluded conformation during active drug transport. Nat Commun, 16, 3619 (2025). https://doi.org/10.1038/s41467-025-58561-4
11.Dwivedi, V. D., Bharadwaj, S., Afroz, S., Khan, N., Ansari, M. A., Yadava, U., Tripathi, R. C., Tripathi, I. P., Mishra, S. K., & Kang, S. G. (2020). Anti-dengue infectivity evaluation of bioflavonoid from Azadirachta indica by dengue virus serine protease inhibition. Journal of Biomolecular Structure and Dynamics, 39(4), 1417–1430. https://doi.org/10.1080/07391102.2020.1734485
12.Fernández-Quintero, M. L., Kokot, J., Waibl, F., Fischer, A.-L. M., Quoika, P. K., Deane, C. M., & Liedl, K. R. (2023). Challenges in antibody structure prediction. MAbs, 15(1). https://doi.org/10.1080/19420862.2023.2175319
13.Halim, S. A., Khan, S., Khan, A., Wadood, A., Mabood, F., Hussain, J., & Al-Harrasi, A. (2017). Targeting dengue virus NS-3 helicase by ligand based pharmacophore modeling and structure based virtual screening. Frontiers in Chemistry, 5, 88. https://doi.org/10.3389/fchem.2017.00088

14.Hollingsworth, S. A., Dror, R. O. (2018). Molecular dynamics simulation for all. Neuron, 99(6), 1129-1143. https://doi.org/10.1016/j.neuron.2018.08.011
15.Huq, A. K. M. M., Roney, M., Dubey, A., Nasir, M. H., Tufail, A., Aluwi, M. F. F. M., Ishak, W. M. W., Islam, M. R., & Tajuddin, S. N. (2024). Phenolic compounds of Theobroma cacao L. show potential against dengue RdRp protease enzyme inhibition by In-silico docking, DFT study, MD simulation and MMGBSA calculation. PloS one, 19(3), e0299238.
https://doi.org/10.1371/journal.pone.0299238
16.Islam, M. T., Aktaruzzaman, M., Saif, A., Akter, A., Bhat, M. A., Hossain, M. M., Alam, S. M. N., Rayhan, R., Rehman, S., Yaseen, M., & Raihan, M. O. (2025). In silico-based identification of natural inhibitors from traditionally used medicinal plants that can inhibit dengue infection. Molecular Biotechnology, 67(6), 2382–2398. https://doi.org/10.1007/s12033-024-01204-8
17.Jiménez De Oya, N., Esler, W. P., Huard, K., El-Kattan, A. F., Karamanlidis, G., Blázquez, A.-B., Ramos-Ibeas, P., Escribano-Romero, E., Louloudes-Lázaro, A., Casas, J., Sobrino, F., Hoehn, K., James, D. E., Gutiérrez-Adán, A., Saiz, J.-C., & Martín-Acebes, M. A. (2019). Targeting host metabolism by inhibition of acetyl-coenzyme A carboxylase reduces flavivirus infection in mouse models. Emerging Microbes & Infections, 8(1), 624–636.
https://doi.org/10.1080/22221751.2019.1604084
18.Jung, E., Nam, S., Oh, H., Jun, S., Ro, H., Kim, B., Kim, M., Go, Y. Y. (2019). Neutralization of acidic intracellular vesicles by niclosamide inhibits multiple steps of the dengue virus life cycle in vitro. Scientific Reports, 9(1). https://doi.org/10.1038/s41598-019-45095-1
19.Kiemel, D., Kroell, A. H., Denolly, S., Haselmann, U., Bonfanti, J. F., Andres, J. I., Ghosh, B., Geluykens, P., Kaptein, S. J. F., Wilken, L., Scaturro, P., Neyts, J., Van Loock, M., Goethals, O., & Bartenschlager, R. (2024). Pan-serotype dengue virus inhibitor JNJ-A07 targets NS4A-2K-NS4B interaction with NS2B/NS3 and blocks replication organelle formation. NatureCommunications. 15(1): 6080. https://doi.org/10.1038/s41467-024-50437-3
20.Klimoszek, D., Jeleń, M., Dołowy, M., & Morak-Młodawska, B. (2024). Study of the lipophilicity and ADMET parameters of new anticancer diquinothiazines with pharmacophore substituents. Pharmaceuticals, 17(6), 725. https://doi.org/10.3390/ph17060725
21.Kumar, M., Rathore, R. S. (2025). RamPlot: A webserver to draw 2D, 3D, and assorted Ramachandran (φ, ψ) maps. Journal of Applied Crystallography, 58(3), 630-636.
https://doi.org/10.1107/S1600576725001669
22.Lee, I. G., Lee, J., Hong, S. H., & Seo, Y. J. (2023). Apigenin's therapeutic potential against viral infection. Frontiers in Bioscience (Landmark edition), 28(10), 237.
https://doi.org/10.31083/j.fbl2810237
23.Lim, L., Dang, M., Roy, A., Kang, J., Song, J. (2020). Curcumin allosterically inhibits the dengue NS2B-NS3 protease by disrupting its active conformation. ACS Omega, 5(40), 25677–25686. https://doi.org/10.1021/acsomega.0c00039
24.Lipinski, C. A. (2004). Lead- and drug-like compounds: the rule-of-five revolution. Drug Discovery Today: Technologies, 1(4), 337-341. https://doi.org/10.1016/j.ddtec.2004.11.007
25.Mesmar, J., Abdallah, R., Badran, A., Maresca, M., Shaito, A., & Baydoun, E. (2022). Ziziphus nummularia: A comprehensive review of its phytochemical constituents and pharmacological properties. Molecules, 27(13): 4240. https://doi.org/10.3390/molecules27134240
26.Mustahil, N. A., Sukari, M. A., Abdul, A. B., Ali, N. A., Lian, G. E. C. (2013). Evaluation of biological activities of Alpinia mutica Roxb. and its chemical constituents. Pakistan Journal of Pharmaceutical Sciences, 26(2), 391-395.
27.Nie, S., Yao, Y., Wu, F., Wu, X., Zhao, J., Hua, Y., Wu, J., Huo, T., Lin, Y. L., Kneubehl, A. R., Vogt, M. B., Ferreon, J., Rico-Hesse, R., & Song, Y. (2021). Synthesis, structure-activity relationships, and antiviral activity of allosteric inhibitors of flavivirus NS2B-NS3 protease. Journal of Medicinal Chemistry, 64(5), 2777–2800. https://doi.org/10.1021/acs.jmedchem.0c02070
28.Owen, L., Laird, K., & Shivkumar, M. (2022). Antiviral plant-derived natural products to combat RNA viruses: Targets throughout the viral life cycle. Letters in Applied Microbiology, 75(3): 476–499. https://doi.org/10.1111/lam.13637
29.Pražnikar, J., Tomić, M., & Turk, D. (2019). Validation and quality assessment of macromolecular structures using complex network analysis. Scientific Reports, 9(1). https://doi.org/10.1038/s41598-019-38658-9
30.Priyono, Q. A. P., Yusniasari, P. A., Alifiansyah, M. R. T., Suryanto, G. Y., Widyowati, R., Herdiansyah, M. A., Ansori, A. N. M., Purnobasuki, H., Pratiwi, I., Makhmudov, F., Azimova, S., Kizatova, M., Rebezov, M., Jakhmola, V., Sahadewa, S., Durry, F. D. (2024). Ethnomedical potentials,

phytochemicals, and medicinal profile of Alpinia galanga L.: A comprehensive review. Bio-Integration, 5(1): 1-12. https://doi.org/10.15212/bioi-2024-0032.
31.Rahayu, S., Rohmatika, A. U., Islamatasya, U., Herdiansyah, M. A., Susilo, R. J. K., Hayaza, S., Santoso, D., Anggarda, O. Y., Wahyuningsih, S. P. A., Darmanto, W. (2025). Potential of Ganoderma applanatum extract as anticancer and immunomodulator in diethylnitrosamine-induced colon cancer. Tropical Journal of Natural Product Research, 9(9), 4310-4320. https://doi.org/10.26538/tjnpr/v9i9.29
32.Sarwar, M. W., Riaz, A., Dilshad, S. M. R., Al-Qahtani, A., Nawaz-Ul-Rehman, M. S., & Mubin, M. (2018). Structure activity relationship (SAR) and quantitative structure activity relationship (QSAR) studies showed plant flavonoids as potential inhibitors of dengue NS2B-NS3 protease. BMC Structural Biology, 18(1), 6. https://doi.org/10.1186/s12900-018-0084-5
33.Taib, M. N. A. M., Anuar, N., Hanafiah, K. M., Al-Shammary, A. A. K., Saaid, M., Awang, K. (2020). Chemicals constituents isolated from cultivate Alpinia conchigera griff. and antimicrobial activity. Tropical Life Sciences Research, 31(1), 159-178. https://doi.org/10.21315/tlsr2020.31.1.10
34.Tuccinardi, T. (2021). What is the current value of MM/PBSA and MM/GBSA methods in drug discovery?. Expert opinion on drug discovery, 16(11), 1233-1237.
https://doi.org/10.1080/17460441.2021.1942836
35.Villaflores, O. B., Macabeo, A. P. G., Gehle, D., Krohn, K., Franzblau, S. G., Aguinaldo, A. M. (2010). Phytoconstituents from Alpinia purpurata and their in vitro inhibitory activity against Mycobacterium tuberculosis. Phcog Mag, 6(24), 339-344. https://doi.org/10.4103/0973-1296.71785
36.Vora, J., Patel, S., Athar, M., Sinha, S., Chhabria, M. T., Jha, P. C., & Shrivastava, N. (2020). Pharmacophore modeling, molecular docking and molecular dynamics simulation for screening and identifying anti-dengue phytocompounds. Journal of Biomolecular Structure and Dynamics, 38(6), 1726–1740. https://doi.org/10.1080/07391102.2019.1615002
37.Wiradana, P. A., Wiartini, N. W. A., Sucipto, T. H., Herdiansyah, M. A., Permatasari, A. A. A. P., Widhiantara, I. G., Sari, N. K. Y., Darmanto, W., Panjaitan, N. S. D., Kusala, M. K. J. (2025). Evaluation of mangrove, Acanthus ilicifolius aqueous extract on inhibition of dengue virus replication: in vitro and molecular docking approach. Indonesian Journal of Tropical and Infectious Disease, 13(3), 251-266. https://doi.org/10.20473/ijtid.v13i3.71217
38.World Health Organization. (2025). Dengue: Global Situation, Surveillance and Progress – 2024 Update. Weekly Epidemiological Record 52. Available at:
https://www.who.int/publications/i/item/who-wer10052-665-678 (11.06.26).
39.Yang, J., Xu, Y., Yan, Y., Li, W., Zhao, L., Dai, Q., Li, Y., Li, S., Zhong, J., Cao, R., & Zhong, W. (2020). Small molecule inhibitor of ATPase activity of HSP70 as a broad-spectrum inhibitor against flavivirus infections. ACS Infectious Diseases, 6(5), 832–843.
https://doi.org/10.1021/acsinfecdis.9b00376
40.Zhakipbekov, K., Turgumbayeva, A., Akhelova, S., Bekmuratova, K., Blinova, O., Utegenova, G., Shertaeva, K., Sadykov, N., Tastambek, K., Saginbazarova, A., Urazgaliyev, K., Tulegenova, G., Zhalimova, Z., & Karasova, Z. (2024). Antimicrobial and other pharmacological properties of Ocimum basilicum, Lamiaceae. Molecules. 29(2): 388. https://doi.org/10.3390/molecules29020388